Vibrational spectroscopy and soft-mode behavior in Rochelle salt

S. Kamba* and G. Schaack
Physikalisches Institut der Universität Würzburg, Am Hubland, D-97074 Würzburg, Germany

J. Petzelt
Institute of Physics, Czech Academy of Sciences, Na Slovance 2, 180 40 Prague 8, Czech Republic
(Received 16 January 1995)

A complete set of the far-infrared transmission and reflection spectra of Rochelle salt together with Raman spectra were obtained in the broad temperature range between 15 and 300 K. All observed phonons below 700 cm^{-1} were classified according to their types of symmetry. The temperature dependence of the soft-mode frequency ($\sim$20 cm^{-1} at 30 K and $\sim$0.15 cm^{-1} at T_{C1} = 255 K) and the soft-mode oscillator strength (ten times higher at T_{C1} than at low temperatures) was explained by coupling of the mode near 75 cm^{-1} which partially softens with infrared inactive hard modes at 37 and 13 cm^{-1} of the same symmetry. The dynamical origin of the phase transitions in Rochelle salt is therefore not the soft relaxation observed in microwave and near-millimeter spectra in a restricted temperature range around T_{C1} and T_{C2} = 297 K, but softening of the optical phonon near 75 cm^{-1}. The phase transitions in Rochelle salt can be treated as a mixture of displacive and order-disorder type.

I. INTRODUCTION

Rochelle salt $NaKC_4H_4O_6{\cdot}4H_2O$ (RS) is the first known ferroelectric.[1] Although RS was studied by many authors within the last 70 years, the understanding of the mechanism leading to the formation of a state with a spontaneous polarization is still incomplete. In contrast to all other ferroelectrics, its ferroelectric phase (space group $P2_1$-C_2^2, $Z = 4$) exists only between T_{C1} = 255 K and T_{C2} = 297 K. Above and below these temperatures RS is paraelectric (space group $P2_12_12$-D_2^3, $Z = 4$).[2] The spontaneous polarization in the monoclinic ferroelectric phase was explained at first by means of spontaneous orienting of hydrogen bonds,[3] because the hydrogen bonds between the molecules of water of crystallization and the oxygen atoms of the anions are oriented almost parallel to the ferroelectric a axis. However, Frazer[4] observed later that the phase transitions (PT's) are associated with reorientations of one of the hydroxyl groups of the tartrate molecules and the ferroelectric properties arise from the associated dipoles. More recently, Iwata *et al.* performed a neutron diffraction experiment and observed that not only some atomic groups but the molecules as a whole are disordered in the paraelectric phase with a small disordering amplitude.[5]

A Debye relaxation mode was observed in the microwave region and its relaxation frequency linearly softens with temperature near T_{C1} and T_{C2};[6–8] therefore the PT's were regarded as classical examples of the order-disorder type. However, several years ago an unusual behavior of the soft relaxation was observed in the near-millimeter region (4–24 cm^{-1}) at low temperatures.[9] Its relaxation frequency at temperatures between 180 and 230 K no longer follows a linear temperature dependence observed in the vicinity of T_{C_1} but obeys essentially a cubic law with the extrapolated softening temperature in the middle between T_{C1} and T_{C2}. At temperatures below 180 K the mode hardens more slowly and exhibits a resonant rather than relaxation behavior. Finally, at 5 K the mode is strongly underdamped and has a frequency of $\approx$ 21 cm^{-1}. Because its oscillator strength is reduced on cooling by one order of magnitude, Volkov *et al.*[10] suggested that this mode is probably linearly coupled with another optical phonon in the far-infrared (FIR) range. Based on the experimental results,[9] Volkov *et al.*[10] concluded that the transition at T_{C1} is more likely displacive than order-disorder.

Recent dielectric measurements[11] in the 1–35.8 GHz range revealed an additional relaxation mode in the microwave region. Its relaxation frequency hardens linearly on cooling below T_{C1} and its relaxation strength decreases at lower temperatures and practically disappears below 120 K from the spectra. This relaxator coexists in the spectra with the insufficiently softened optical mode near 20 cm^{-1}. This is in contrast to the results of Volkov *et al.*,[9,10] who observed only one soft mode and its strongly nonlinearly temperature dependent frequency and oscillator strength interpreted by the coupling with an optical phonon from the higher frequency region.

For the proof or disproof of Volkov's model, FIR and Raman spectra are desirable in a broad temperature range. It is surprising that up to now only two incomplete sets of low temperature FIR transmission spectra ($E \| a, b$ spectra below 250 cm^{-1} at 80 K and the same symmetry spectra below 110 cm^{-1} at 7 and 80 K) were published.[12,13] The polarized middle- and near-infrared spectra of RS near T_{C2} were published in Refs. 14 and 15. The detailed temperature dependence of FIR transmission and reflection spectra of RS in the temperature

0163-1829/95/51(21)/14998(10)/$06.00

range between 15 and 300 K was, according to the authors' knowledge, never published. Some Raman measurements have been published (for example, Refs. 16 and 17), but the majority of these papers only present data at high temperatures near the PT's. Only one low temperature (2 K) spectrum of A symmetry was published by Winterfeldt.[16] The expected soft mode which should couple with the mode near 21 cm^{-1} should have B_3 symmetry and therefore should be IR active for polarization $E \parallel a$ and Raman active in the bc component of the polarizability tensor.[16]

The aim of this paper is to present FIR transmission and reflection spectra of all three polarizations in the range from 10 to 650 cm^{-1} at temperatures between 15 and 300 K and Raman spectra of all symmetries in the same temperature range. The anomalous temperature dependences of the observed phonon frequencies are discussed using the model of the coupled hard and soft modes.

II. EXPERIMENTAL DETAILS

Plane-parallel RS samples of (001) and (010) orientation were cut and polished from a single crystal of several cm^3 of very good optical quality. The diameter of the plates was about 10 mm, the thickness was varied between 95 μm and 1.2 mm for FIR transmission, 1.5-2 mm for FIR reflection, and ~3.5 mm for Raman measurements. The crystal orientation was determined by visual identification of the natural growth faces and refined by x-ray diffraction and a polarizing microscope.

FIR reflection and transmission spectra of $E \parallel a, b, c$ polarizations were performed using a Grubb Parsons Fourier spectrometer with a liquid-helium-cooled Si bolometer with a resolution of 1.2 cm^{-1} in the 100–650 cm^{-1} range and with a resolution of 0.6 cm^{-1} in the 10–100 cm^{-1} range. Because of the dehydration of the crystal in vacuum the samples were measured under normal pressure in helium atmosphere.

Raman scattering spectra were taken at temperatures between 40 and 300 K in the frequency range from 5 to 700 cm^{-1} with a Dilor XY spectrometer equipped with a liquid nitrogen cooled charge-coupled device (CCD) detector. All the spectra of cc, ba, ca, and bc symmetry were taken in the 90° scattering geometry $a(\ldots)b$.

III. DATA EVALUATION

All the IR spectra were fitted with a superposition of classical oscillators and in the case of $E||a$ with an additional Debye relaxator in which case the complex dielectric function ε^* at frequency ω has the form

$$\varepsilon^*(\omega) = \varepsilon_\infty + \sum_{i=1}^{n} \frac{\Delta\varepsilon_i \omega_i^2}{\omega_i^2 - \omega^2 + i\omega\gamma_i} + \frac{\Delta\varepsilon_R \omega_R}{\omega_R + i\omega}. \quad (1)$$

Here ε_∞ is the permittivity at frequencies much higher than all transverse oscillator mode eigenfrequencies ω_i, γ_i is the damping of the ith oscillator, ω_R is the relaxation frequency, and $\Delta\varepsilon_i$ and $\Delta\varepsilon_R$ denote the contributions of the ith oscillator and relaxator to the static permittivity, respectively. In addition to it, the low frequency part of the $E \parallel a$ spectra was fitted with the dielectric function due to a pair of coupled oscillators[19,20]

$$\varepsilon^*(\omega) = \frac{s_1(\omega_2^2 - \omega^2 + i\omega\gamma_2) + s_2(\omega_1^2 - \omega^2 + i\omega\gamma_1) - 2\sqrt{s_1 s_2}(\alpha + i\omega\gamma)}{(\omega_1^2 - \omega^2 + i\omega\gamma_1)(\omega_2^2 - \omega^2 + i\omega\gamma_2) - (\alpha + i\omega\gamma)^2}, \quad (2)$$

where $s_i = \Delta\varepsilon_i \omega_i^2$ $(i = 1, 2)$ is the oscillator strength of the ith oscillator. The real coupling constant α renormalizes the eigenfrequencies ω_1 and ω_2 to[19]

$$\omega_\pm^2 = \frac{1}{2}(\omega_1^2 + \omega_2^2) \pm \sqrt{\frac{1}{4}(\omega_1^2 - \omega_2^2)^2 + \alpha^2}. \quad (3)$$

α has to fulfill the stability condition $|\alpha| \leq \omega_1\omega_2$. The imaginary coupling constant γ describes the mutual damping of both oscillators. The reflectivity was then calculated from the formula[21]

$$R(\omega) = \left| \frac{\sqrt{\varepsilon^*(\omega)} - 1}{\sqrt{\varepsilon^*(\omega)} + 1} \right|^2. \quad (4)$$

The formula for the transmitted intensity T taking interferences in the crystal slab into account is given by[21]

$$T(\omega) = \frac{\exp[-K(\omega)d]\{[1 - R(\omega)]^2 + 4R(\omega)\sin^2\Theta(\omega)\}}{\{1 - R(\omega)\exp[-K(\omega)d]\}^2 + 4R(\omega)\sin^2[\Theta(\omega) + \beta(\omega)]\exp[-K(\omega)d]}. \quad (5)$$

The angle $\beta = \frac{\omega n d}{c}$ indicates the phase change due to one passage through the plate. The angle $\Theta = \arctan(\frac{2k(\omega)}{n^2(\omega)+k^2(\omega)-1})$ describes the phase shift between the incident and reflected waves after one reflection. The absorption coefficient K is defined by $K = \frac{2\omega k}{c}$, c being the velocity of the light in vacuum. $n = \left(\frac{1}{2}[(\varepsilon'^2 + \varepsilon''^2)^{1/2} + \varepsilon']\right)^{1/2}$ and $k = \left(\frac{1}{2}[(\varepsilon'^2 + \varepsilon''^2)^{1/2} - \varepsilon']\right)^{1/2}$ signify the refraction index and extinction coefficient, respectively.

IV. RESULTS AND DISCUSSION

In Figs. 1 and 2 we present the IR reflection and transmission spectra of RS for all three polarizations $E\|a, b, c$ at several temperatures between 15 and 300 K. All the spectra were measured in the region from 10 to 650 cm^{-1}, but below 100 cm^{-1} the samples are partially transparent and reflection spectra are affected by the reflection from the back surface and from the metal sample holder behind the sample. Therefore in Fig. 1 we present only the reflectivity spectra above 100 cm^{-1}. In Fig. 3, we show the $E\|a$ reflection spectra below 100 cm^{-1} together with their fits. These spectra are discussed in more detail below. It is generally true that below 100 cm^{-1} the transmission spectra (see Fig. 2) yield more accurate optical constants than does the reflectivity. At higher frequencies the samples are opaque or semitransparent at most. An example of the latter case is demonstrated in Fig. 4 for the ferroelectric polarization $E\|a$. Note the appearance of the mode near 300 cm^{-1} below 200 K. Its damping increases strongly with increasing temperature, causing its apparent vanishing at high temperatures without strong temperature changes of its strength.

The apparent changes in the intensities of all reflection and transmission bands with temperature are mostly caused by the dramatic increase of the phonon damping with temperature. At high temperatures all modes are heavily damped. Consequently it is impossible to distinguish the new IR active modes in the ferroelectric phase from modes active in the low temperature paraelectric phase. Therefore we have focused our studies mostly on the low temperature paraelectric phase.

Periodic oscillations in the transmission spectra are caused by interferences due to the plane-parallel sample surfaces. Clear distinction of absorption bands from interferences in the transmission spectra was possible by using samples with different thicknesses. As an example, in Fig. 5 we have plotted FIR transmission spectra of $E\|a$ polarization at 15 K for three different sample thicknesses. The interferences are distinctly seen in the region below 20 and between 25 and 70 cm^{-1}; the other minima in the spectra are phonon absorption bands. The interferences are not distinct in the spectrum of the thick sample ($d = 1180$ μm) due to the finite spectral resolution (0.6 cm^{-1}) used.

Gerbaux *et al.*[13] stated that the absorptivity of RS below 50 cm^{-1} and below 80 K does not increase with the sample thickness according to Beer's law, but the transmission is rather independent of the sample thickness.

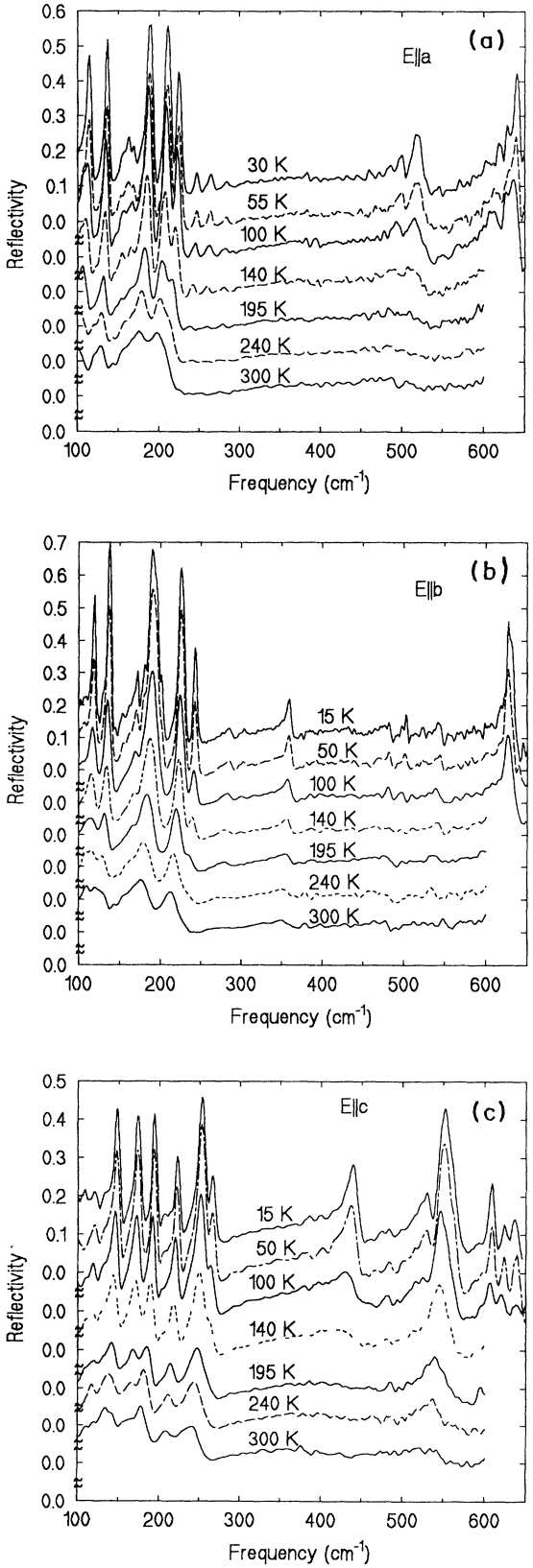

FIG. 1. FIR reflectivity spectra of RS at various temperatures for (a) $E\|a$, (b) $E\|b$, and (c) $E\|c$ polarizations. The spectra above 600 cm^{-1} were measured only below 100 K.

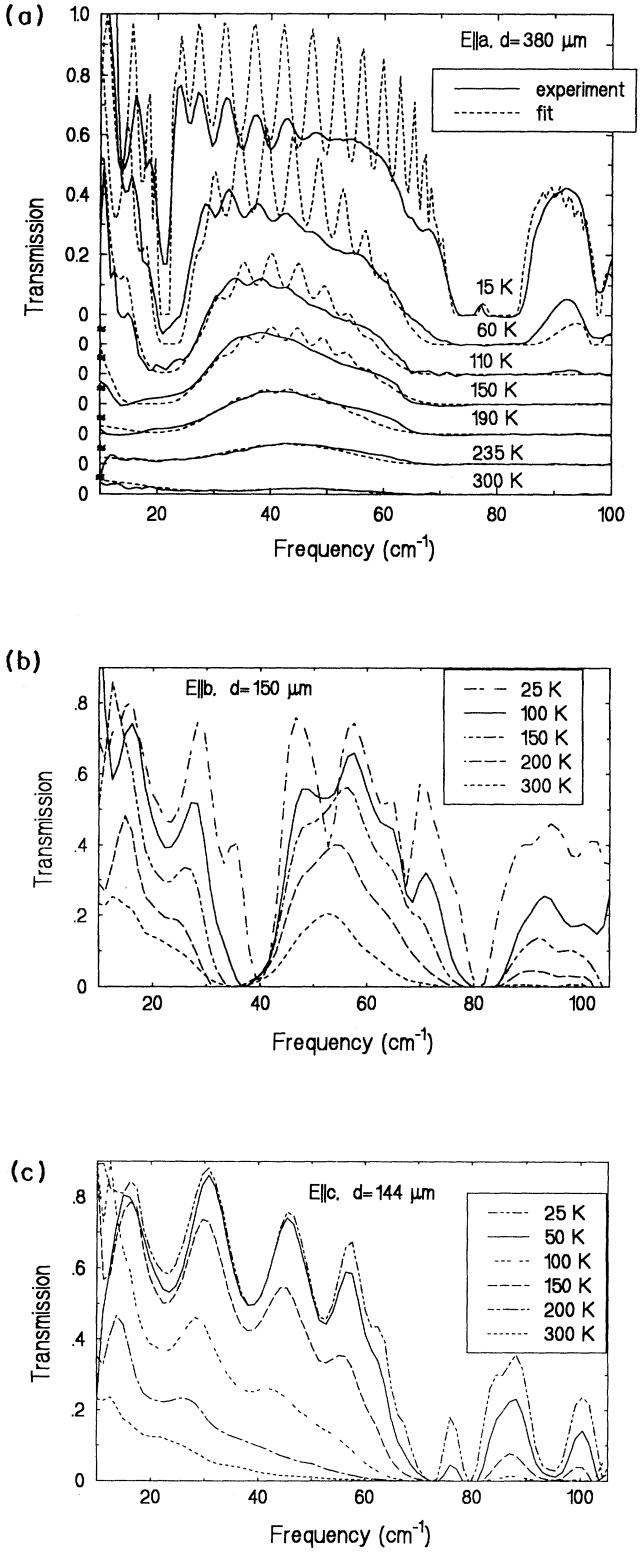

FIG. 2. Temperature dependence of the FIR transmission spectra for (a) $E||a$ (broken lines are results of the coupled-oscillator fit), (b) $E||b$, and (c) $E||c$ polarizations. At low temperatures (high transmission) interferences in the spectra are evident.

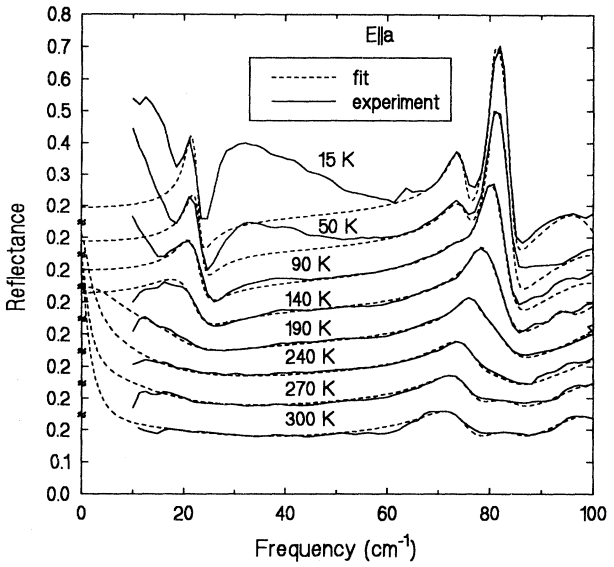

FIG. 3. FIR reflection spectra below 100 cm^{-1} for $E \parallel a$ polarization. Solid lines are experimental curves, broken lines are the result of the fit with the sum of classical uncoupled oscillators plus two coupled oscillators (see Tables II and III). Note the discrepancy between experimental reflectance and the fitted value at low temperatures below 60 cm^{-1} caused by the back surface reflection (the thickness of the sample was $\sim$ 1.5 mm) due to partial transparency of the sample.

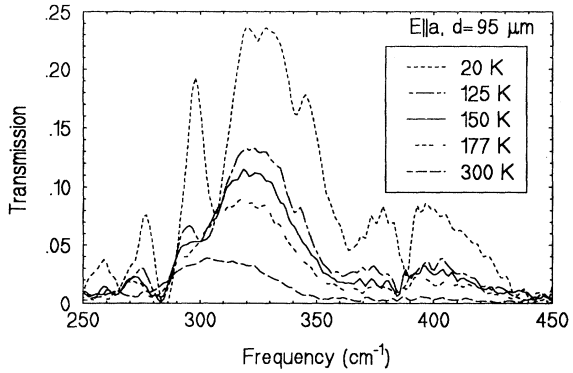

FIG. 4. Temperature dependence of the FIR transmission spectra for $E \parallel a$ polarization.

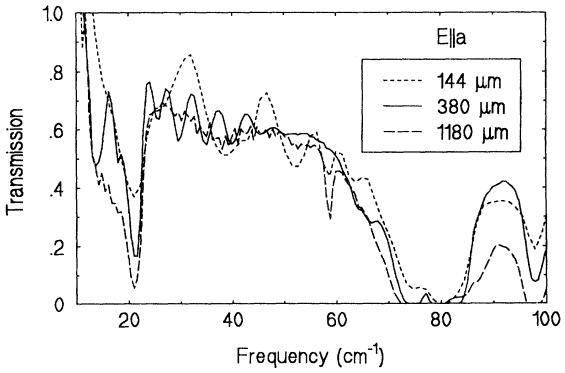

FIG. 5. FIR transmission spectra of $E \parallel a$ polarization at 15 K for three different sample thicknesses.

They interpret their observation by a new PT undergone at low temperatures in the bulk of the sample but not in the surface layer. They claim that the bulk of the sample does not absorb below this PT but the surface layers do. We have clearly observed that the transmission in the range near 20 cm^{-1} is dependent on the sample thickness (see Fig. 5). The transmission in the range from 30 to 60 cm^{-1} is practically independent of the thickness (except for the interferences) which is due to the negligible absorption at these frequencies. Therefore we can state that the assumption of the absorbing surface layers[13] and the new PT below 80 K in RS is not confirmed.

Factor-group analysis and selection rules for the lattice vibrations in the paraelectric phase of RS yield[16,17,22]

$$\Gamma = 83A(a^2, b^2, c^2) + 82B_1(c, ab) + 84B_2(b, ac) + 84B_3(a, bc) + (B_1 + B_2 + B_3)_{\text{acoustic}} .$$

It means that the A modes are only Raman active while the B_1, B_2, and B_3 modes are both IR and Raman active.

In Fig. 6 Raman spectra of all symmetries are shown at three different temperatures, at 300 K in the high temperature paraelectric phase and at 200 and 40 K in the low temperature paraelectric phase. No spectra of the ferroelectric phase are presented in Fig. 6 because no important changes with respect to those in the paraelectric phase were observed. Detailed spectra of Raman scattering near both PT's were already published in Ref. 16. Winterfeldt's published A-symmetry spectra[16] are exactly the same as our $a(cc)b$ spectra but they differ from Taylor *et al.*'s $c(aa)b$ spectra.[17] This difference is caused by different mode strength in cc and aa spectra although all modes have the same A symmetry. Because of the heavy damping at high temperatures, it is impossible to resolve all modes constituting the broad Raman bands. At low temperatures many new modes appear in our spectra due to the reduced damping. The new modes do not originate from a new PT. The PT in RS at 212 K suggested by Ushatkin *et al.*[23] on the basis of a dielectric anomaly in the submillimeter region was not confirmed later (for example, Ref. 24). This anomaly was easily explained by hardening of the soft mode on cooling.[9]

From the symmetry point of view, the B_i modes ($i = 1, 2, 3$) are both Raman and IR active. Many modes were actually observed in both types of spectra but not all of them. In general, the modes of the same symmetry will have a different strength in different types of spectra; therefore some of the modes were observed only in one type of spectra. The list of all modes observed at 40 K is presented in Table I. The frequencies of the modes observed by Malineau *et al.*[12] at 81 K in IR spectra below 245 cm^{-1} at $E\|a, b$ polarizations correspond very well to our spectra. However, the resolution of these spectra was lower than ours; therefore we see more modes. Low temperature IR spectra below 110 cm^{-1} were published also in Ref. 13. The positions of all absorption bands correspond well to our data, except for the bands at 53 ($E\|b$) and 57 cm^{-1} ($E\|a$). We do not see the former band and the latter one was observed in our spectra only in the transmission spectrum of the thick sample ($d = 1.18$ mm). IR spectra at $E\|c$ polarization are also presented

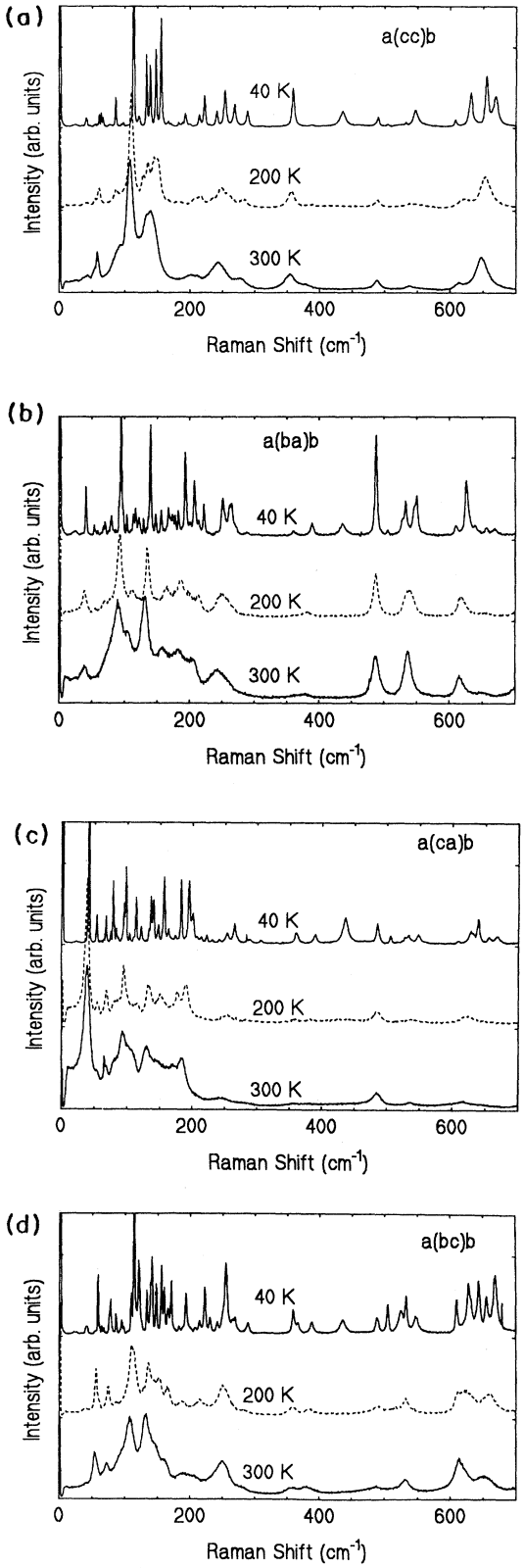

FIG. 6. Raman spectra of (a) cc, (b) ba, (c) ca, and (d) bc symmetries at three different temperatures in the paraelectric phase. A huge increase of the number of modes due to the decrease of mode damping at low temperatures is apparent.

TABLE I. Phonon mode frequencies of different symmetries in RS observed at 40 K (in cm^{-1}) in infrared (a, b, c) or/and Raman (cc, ba, ca, bc) spectra. Frequencies are obtained from the uncoupled-oscillator model.

A	B_1	Spectrum	B_2	Spectrum	B_3	Spectrum
cc						
61.1	70.5	c, ba	41.2	b, ca	21.6	a
64.6	79.8	c, ba	53.6	ca	58.6	a, bc
67.0	94.8	c, ba	67.7	b, ca	64.2	bc
86.7	103.5	c, ba	75.2	ca	74.0	a
114.0	117.3	c, ba	79.2	b, ca	80.5	a, bc
122.3	122.0	c, ba	83.6	ca	86.4	bc
133.7	129.0	ba	95.4	ca	98.0	a, bc
139.2	139.7	c, ba	98.0	ca	109.4	bc
148.2	147.5	c, ba	104.2	ca	113.8	a, bc
156.1	167.8	ba	109.0	b	118.5	a
166.8	174.0	c, ba	113.5	ca	121.0	bc
188.7	193.7	c, ba	121.3	b, ca	133.4	bc
193.0	207.7	ba	125.0	b	141.0	a, bc
214.8	214.0	ba	136.3	b, ca	147.8	a, bc
222.7	222.0	c, ba	140.0	ca	155.6	bc
241.7	251.0	c, ba	156.3	b, ca	160.0	bc
254.2	264.4	c, ba	163.4	b, ca	165.9	a, bc
269.1	293.0	c, ba	174.0	b, ca	170.8	a, bc
289.4	313.0	c	182.7	b, ca	188.6	a, bc
359.9	389.0	c, ba	192.0	b, ca	193.6	bc
436.4	436.0	c, ba	205.5	b, ca	201.0	a
490.9	488.0	ba	209.0	b	209.0	a
547.4	533.3	c, ba	213.0	ca	214.5	bc
608.5	550.5	c, ba	222.7	b, ca	222.4	a, bc
631.8	609.8	c, ba	241.4	b, ca	230.4	bc
656.0	626.4	c, ba	265.0	ca	254.8	bc
669.6	638.9	c, ba	288.0	b, ca	265.4	a, bc
	656.3	ba	306.2	b, ca	289.0	a, bc
	668.8	ba	360.7	b, ca	305.5	a
			389.0	b, ca	359.3	bc
			436.0	b, ca	366.1	a, bc
			470.0	b	387.9	a, bc
			485.0	b, ca	436.0	bc
			505.8	b, ca	489.0	bc
			527.9	b, ca	505.1	a, bc
			533.3	ca	525.4	a, bc
			548.7	b, ca	532.6	bc
			629.3	b, ca	548.2	bc
			639.7	ca	610.1	a, bc
			655.5	ca	628.3	a, bc
			668.4	ca	643.9	bc
					655.3	bc
					668.8	bc

here.

The highest number of the modes lies below $\sim$ 300 cm^{-1} (Figs. 1 and 6). The external modes [vibrations of the whole molecular entities, i.e., H_2O and $C_4H_4O_6^{2-}$ ions (tartrate)] lie mostly below $\sim$ 200 cm^{-1}, but the internal vibrations like bond bending of C(OH) groups, angle deformations of C-C-C chains, and CC twist are also present in this range.[18,22,25] The modes at higher frequencies are mostly internal vibrations (angle deformations, bond bending, stretching, and torsions of tartrate groups and water molecules); however libration frequencies of crystal water lie also in this range.[25] At high temperatures this libration band is weak and broad, but at low temperatures it becomes intense in all types of spectra and has a well defined frequency of 436 cm^{-1} (see Fig. 6). The detailed assignment of all the modes observed in Raman and IR spectra at high temperatures was already published in Refs. 18, 22, 25; and therefore we do not present it here.

V. SOFT-MODE BEHAVIOR

If Volkov's theory[10] of coupled oscillators is valid, we should find one optical phonon of B_3 symmetry with an anomalous temperature behavior. The soft mode near 20 cm^{-1} (active in $E\|a$ spectra) is not seen in our Raman spectra of B_3 symmetry. All Raman active modes have the usual temperature dependences; their frequencies increase only slightly at low temperatures. Let us, therefore, investigate the $E\|a$ FIR spectra. Practically all modes clearly demonstrate the usual hardening on cooling [see Figs. 1(a) and 3]. Only two modes at 74 and 81 cm^{-1} (frequencies at 15 K) behave differently. The former mode hardens on heating in contrast to all other modes and the latter softens; therefore they undergo an anticrossing at $\sim$ 160 K (see Fig. 3). Crossing is forbidden because of the same symmetry type of both modes. The mode near 20 cm^{-1} is an underdamped oscillator at low temperatures and becomes overdamped at high temperatures and softens.

For a more accurate fit at low frequencies we have used not only our FIR transmission and reflection spectra, but also published near-millimeter spectra from Ref. 9, microwave data (1–36 GHz) from Ref. 11, and not yet published continuous dielectric spectra in the range of 0.1 to 10 GHz at temperatures between 240 K and 312 K, which were kindly provided to us by Horioka.[26]

The absorption and reflection bands above 70 cm^{-1} were fitted with the superposition of classical oscillators [Eq. (1)], but the lower frequency part of the spectra was fitted with several different models.

A. Uncoupled-oscillator model

All FIR reflection spectra could be fitted very well with this model, but the parameters of the soft mode near 20 cm^{-1} have unusual temperature dependences. The eigenfrequency softens on heating from 21.7 to $\sim$ 13 cm^{-1}, the damping increases from 2 (at 30 K) to $\sim$ 60 cm^{-1} (at 300 K), and oscillator strength increases from $\sim$ 400 (30 K) to $\sim$ 4000 cm^{-2} (300 K). This result is in a qualitative agreement with Refs. 9 and 10, but the fit of FIR transmission was not successful with the same parameters. The oscillator strength is so high that a sample of the thickness chosen in the experiment shows a much lower transparency than observed. It was impossible to fit the microwave data[11,26] with the same oscillator model. Therefore we tried to replace the soft oscillator by a Debye relaxator at high temperatures.

B. Relaxator model at high temperatures

In this case we have fitted the low frequency part of the spectra at high temperatures not with an overdamped oscillator, but with a Debye relaxator. The relaxation in microwave[11,26] and near-millimeter[9] spectra was fitted very successfully. However, the fit of the reflectivity was not accurate below 30 cm^{-1} (lower absolute value and different shape of the reflectivity spectra than in the experiment). The fit of the FIR transmission was also not successful. Although the relaxator describes the low FIR transmission at low frequencies and high temperatures, it is not able to fit the transmission minimum at $\sim$ 20 cm^{-1} accurately [Fig. 2(a)]. Therefore we have used both Debye relaxator and soft oscillator for our fit [Eq. (1)].

C. Model of a combined Debye relaxator and oscillator

The relaxator describes very well the dielectric anomaly in microwave and near-millimeter spectra at high temperatures above 190 K. However, it practically disappears from the spectra below 140 K (small relaxation strength, Fig. 7). The oscillator near 20 cm^{-1} is overdamped at high temperatures, but it transforms into a sharp underdamped oscillator below 100 K. This oscillator is necessary also at high temperatures for the FIR transmission and reflection spectra description [see Figs. 2(a) and 3]. Its oscillator strength is temperature dependent only below 100 K ($\sim$ 200 cm^{-2} at 5 K and $\sim$ 700 cm^{-2} at 90 K—see Fig. 7); it is practically constant above 100 K. The relaxator takes over a part of the oscillator strength from the original one-oscillator fit at high temperatures (Fig. 7). In this case we have supported Horioka's conclusion[11] that two excitations—a slightly overdamped oscillator and a relaxator—coexist

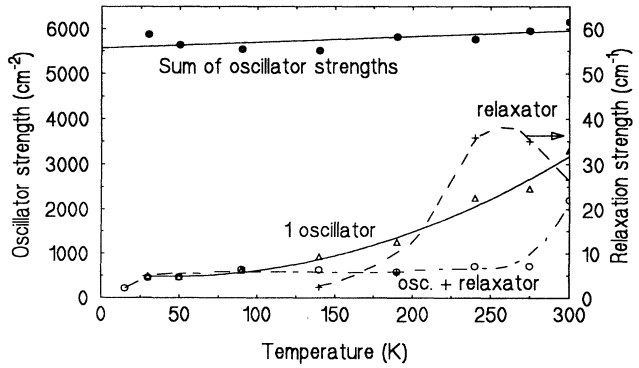

FIG. 7. Temperature dependences of the oscillator strengths of the lowest B_3 mode ($\sim$ 20 cm^{-1}) obtained from the single-oscillator fit (solid line) and from uncoupled-oscillator and relaxator fit (dotted line). The dashed-dotted line describes the temperature dependence of the relaxation strength (from the latter fit) and the broken line shows the sum of the oscillator strengths of all modes below 85 cm^{-1}.

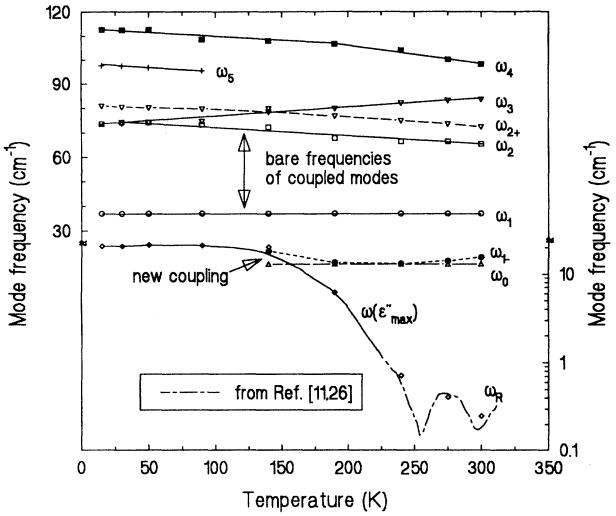

FIG. 8. The temperature dependence of all mode frequencies obtained from the fit of $E\|a$ spectra with coupled-oscillator model and the superposition of uncoupled oscillators (Tables II and III). At low temperatures are coupled only the modes no. 1 and no. 2 (bare frequencies ω_1 and ω_2 are renormalized to ω_{1-} and ω_{2+}). The former mode is coupled above 140 K also with the hard mode no. 0 (bare frequency ω_0). The frequency of the observed maximum of ε''_a below 22 cm^{-1} together with the soft relaxation frequency $\omega_R = \frac{\omega_{0-}^2}{\gamma_{0-}}$ (compared with experimental results in Refs. 11 and 26) are also depicted. Note the change of logarithmic to linear scale at 30 cm^{-1}.

in $E\|a$ spectra at high temperatures. The oscillator eigenfrequency softens only slowly but its damping increases strongly on heating. The relaxation frequency softens practically linearly up to T_{C1} (see Fig. 8).

Is it possible to explain the unusual temperature behavior of the strengths and frequencies of both the oscillator and relaxator by coupling them with an optical phonon in a higher frequency region, as it was already suggested by Volkov *et al.*?[10]

D. Coupling of the soft mode with a hard mode

We attempted to couple the soft optical phonon at 82 cm^{-1} (the bare frequency ω_2 is 74 cm^{-1} at 15 K) with the hard (temperature independent frequency) phonon at the bare frequency ω_1 of 37 cm^{-1}, which is without coupling IR inactive ($\Delta s_1 = 0$). We have considered no mutual damping (imaginary coupling constant $\gamma = 0$) to reduce the number of fitted parameters [see Eq. (2)]. At first, the real coupling constant α_{12} was taken temperature independent ($\alpha_{12} = 2128$ cm^{-2}). The renormalized frequency ω_{1-} of the lower oscillator mode lies in the 20 cm^{-1} region and the mode becomes infrared active (see Fig. 8). It is possible to explain the softening of this mode on heating by the softening of the mode at $\sim$ 74 cm^{-1}. In this way we can explain also the increase

of the oscillator strength of the lower frequency mode. However, this fit is successful only below 140 K. An additional relaxation as in the case B is needed at higher temperatures (Table II).

We believe that it is possible to describe the whole temperature dependence of all the $E\|a$ spectra modes in the following way. The mode near 80 cm^{-1}, which partially softens, is coupled with the infrared inactive ($\Delta s_1 = 0$) hard mode at 37 cm^{-1} and the latter mode is coupled at high temperatures (above 140 K) with another infrared inactive hard mode with frequency near 10 cm^{-1}.

We did not attempt to fit our data above 140 K with a general three-coupled-oscillator model; instead we used again only the two-coupled-oscillator model plus one independent oscillator with a frequency ω_{2+} describing the original soft mode at $\approx$75 cm^{-1}. The mode at 37 cm^{-1} has a renormalized frequency ω_{1-} below 20 cm^{-1} (see Table III and Fig. 8). We used this mode as a soft mode above 140 K with a bare frequency ω_{1-}, which is coupled with the IR inactive mode at $\omega_0 =$ 13 cm^{-1}. On approaching T_{C1} and T_{C2} ω_{1-} softens to ω_0 and the coupling constant increases to the critical value α_{cr} ($|\alpha_{cr}| = \omega_0\omega_{1-}$ which describes the stability limit of the system for which the renormalized frequency $\omega_0 \to \omega_{0-} = 0$). This describes the softening of the latter mode to the microwave region. The renormalized mode is overdamped and describes the soft relaxation observed in Refs. 11 and 26. It should be noted that the high temperature spectra are fitted with temperature independent bare frequency ω_0, oscillator strength s_0 (=0), and with temperature dependent coupling constant α_{01}. The same spectra can be fitted also with temperature independent α_{01}, but with temperature dependent ω_0 and s_0 ($\neq$0).

TABLE II. Parameters of the FIR spectra fit together with the near-millimeter (Ref. 9) and microwave spectra (Refs. 11, 26). Oscillator frequencies ω_i, relaxation frequency $\omega_R = \frac{\omega_{0-}^2}{\gamma_{0-}}$, and dampings γ_i are in cm^{-1}; oscillator strengths $s_i = \Delta\varepsilon_i\omega_i^2$ ($i = 0, 1, 2 \ldots, 5$) and coupling constant α_{12} are in cm^{-2}. Coupling is introduced between the modes no. 1 and no. 2 only. Above 140 K a new relaxation arises in the spectra (mode no. 0). Note that $T_{C1} = 255$ K and $T_{C2} = 297$ K.

T	300 K	275 K	240 K	190 K	140 K	90 K	50 K	30 K
ω_{0-}	1.6	2.1	2.5	9.0	16.2			
ω_R	0.180	0.327	0.607	7.5	15.8			
s_{0-}	380	380	380	380	350			
γ_{0-}	14.2	13.5	10.3	10.8	16.6			
ω_1	37.0	37.0	37.0	37.0	37.0	37.0	37.0	37.0
s_1	0	0	0	0	0	0.0	0.0	0.0
γ_1	37.5	30.0	28.0	21.9	7.4	2.8	2.7	2.1
α_{12}	2128	2128	2128	2128	2128	2128	2128	2171
ω_2	66.7	67.0	68.3	69.8	72.0	73.9	74.3	74.3
s_2	3380	3240	2960	2970	2950	3040	3290	3450
γ_2	3.4	3.0	2.7	2.5	4.5	2.5	1.5	1.0
ω_3	83.9	83.0	81.4	80.8	79.0	76.3	74.3	73.9
s_3	1890	2000	1800	2200	2430	2500	2350	2430
γ_3	13.0	12.6	11.3	9.9	8.2	7.3	5.0	3.3
ω_4	98.4	100.2	104.2	105.5	107.6	108.5	112.7	112.5
s_4	7070	7420	7380	6480	6660	6520	4140	3640
γ_4	15.0	15.0	14.7	10.6	10.0	8.4	4.8	2.1
ω_5				91.7	95.1	96.2	96.4	96.6
s_5				570	700	920	2230	3360
γ_5				8.8	6.0	5.8	4.8	4.5
ε_∞	4.2	4.2	4.2	4.2	4.0	3.9	3.9	3.9

TABLE III. Parameters of the same fit as in Table II for T$\geq$ 140 K. The low frequency relaxation is expressed by the coupling of the modes no. 0 and no.1. Instead of the mode frequency ω_2 the renormalized frequency ω_{2+} is used.

T	300 K	275 K	240 K	190 K	140 K
ω_0	13.0	13.0	13.0	13.0	13.0
ω_R	0.249	0.413	0.716	6.161	8.982
s_0	0.0	0.0	0.0	0.0	0.0
γ_0	22.2	25.6	19.0	15.4	15.1
α_{01}	208.8	172.7	158.0	81.7	80.8
ω_{1-}	16.5	14.1	13.2	13.6	18.2
s_{1-}	2120	1750	1610	1040	750
γ_{1-}	44.5	41.1	28.2	17.0	9.1
ω_{2+}	72.7	73.6	74.8	76.5	77.9
s_{2+}	2730	2700	2560	2340	2310
γ_{2+}	9.3	8.1	7.5	5.7	4.5
ω_3	83.3	83.0	81.4	80.8	79.2
s_3	1300	1510	1590	2440	2450
γ_3	11.0	11.0	11.7	11.7	8.2
ε_∞	4.2	4.2	4.2	4.2	4.0

The parameters of all fits of FIR spectra below 120 cm^{-1} together with the near-millimeter and microwave spectra are presented in Tables II (accurate below 90 K) and III (above 140 K). The contribution of all other phonons to permittivity ε' at higher frequencies is included in ε_∞. A small decrease of ε_∞ at low temperatures is due to the hardening of all modes above 120 cm^{-1}.

The temperature dependence of all mode frequencies from Tables II and III together with the relaxation frequency ω_R from Refs. 11 and 26 are shown in Fig. 8. The mode no. 1 with the frequency ω_{1-} is really IR active above 140 K only due to the coupling of this mode with the mode no. 2; therefore the bare theoretical frequencies ω_1 and ω_2 are depicted also above 140 K. In the case of heavily damped modes the peak frequency of the loss spectra $\varepsilon''(\omega)$ ($= \omega_R = \frac{\omega_{0-}^2}{\gamma_{0-}}$) has a better defined physical meaning than the eigenfrequency of the overdamped oscillator; therefore the relaxation frequencies ω_R are also shown in Tables II and III. Theoretical values of ω_R in Table II are exactly the same as in Refs. 11 and 26. The values of ω_R in Table III are slightly higher due to the inaccurate values of damping γ_0 (dampings γ_0 and γ_{1-} are mutually influenced), but in spite of that our ω_R values correspond very well to the experimental data from Refs. 11 and 26 (see the points in Fig. 8).

The results of the coupled-oscillator fit of FIR transmission and reflection spectra are seen in Figs. 2(a) and 3 (broken lines). The influence of the microwave relaxation at high temperatures on the reflectivity spectra is seen in Fig. 3 only below 10 cm^{-1} (beyond our range of measurements). Very good agreement of our FIR fit with the microwave[26] and near-millimeter spectra[9,27] is seen in Fig. 9.

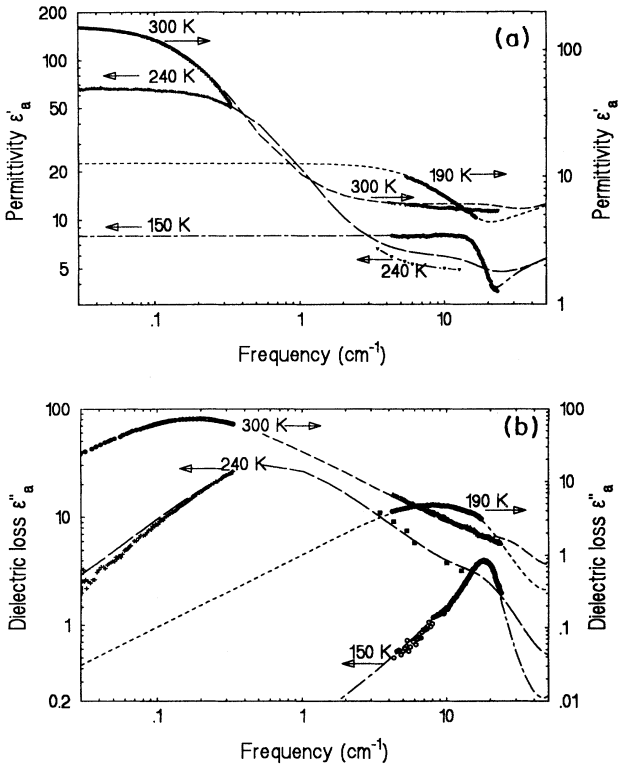

FIG. 9. (a) Permittivity ε'_a and (b) dielectric loss ε''_a of RS in the broad frequency range calculated from the coupled-oscillator fit of FIR spectra (Table III). Theoretical curves are compared with experimental microwave dielectric data below 0.33 cm^{-1} (Ref. 26) and near-millimeter spectra (Ref. 9) (thicker curves and points). Note the double logarithmic scale and two different ordinate scales.

The mode no. 3 has no influence on the phase transitions, but its oscillator strength s_3 is strongly influenced by the anticrossing of this mode with mode no. 2 at 160 K (Fig. 3, Tables II and III). The strengths s_3 are slightly different in Tables II and III due to the different influence of the mode no. 2 in different fit models (independent or coupled oscillator). The sum of the oscillator strengths s_0 (=0), s_{1-}, s_{2+}, and s_3, however, is practically temperature independent (see Fig. 7) in contrast to s_1 from the single-oscillator fit (see Ref. 10 and Fig. 7) where the strength s_1 is ten times higher at high temperatures than at the lowest value. In other words, the summation rule for the IR oscillator strengths is fulfilled for modes below $\sim$ 90 cm^{-1} separately. This means that these modes are essentially decoupled from all the higher frequency modes.

Two modes near 100 cm^{-1} are present in the $E\|a$ spectra in the whole temperature range, but due to the high damping of these modes we were able to resolve them in the spectra only below 190 K. Therefore we have fitted the spectra at high temperatures only with one oscillator (no. 4 in Table II) and with two oscillators (nos. 4 and 5) below 190 K. The oscillator strength s_4 also decreases below 190 K in favor of s_5.

All the modes in Tables II and III are probably external modes (translations and librations) of the tartrate and H_2O molecules, but a more detailed assignment is not possible without any microscopic model.

Kozlov *et al.* explained the PT's in RS by the theory of the double critical point.[28] They fitted very well the temperature dependence of the polarization in the ferroelectric phase, the heat capacity, the effect of pressure on T_{C1} and T_{C2}, and the ultrasound absorption by this model. They proposed also the coupling of a partially softened optical mode with a hard mode. They obtained qualitatively similar temperature dependences of the mode frequencies as we show in Fig. 8 with the only difference that his bare frequency ω_1 agrees with the renormalized frequency ω_{1-} below 200 K. The mode no. 1 is originally IR inactive; its IR activity is only due to the coupling with the mode no. 2. Therefore the bare frequency ω_1 should be higher than ω_{1-} also at low temperatures. Kozlov *et al.* did not propose the coupling of the mode near 20 cm^{-1} with any other relaxational mode; the two-mode behavior in the near-millimeter and microwave region was observed by Horioka *et al.*[11,26] only recently. However, Kozlov *et al.* stressed also the coupling of mode no. 1 with a transverse acoustic phonon due to the piezoeffect, which accounts for the difference between the clamped and free permittivity already observed in Ref. 29.

VI. CONCLUSION

It becomes obvious from the fits of all our FIR transmission and reflection spectra together with the near-millimeter[9,27] and microwave[11,26] spectra found in the literature that a complicated sequence of coupled modes exists in RS. The mode near 75 cm^{-1}, which partially softens, is coupled with the hard mode at 37 cm^{-1} and this mode is coupled above 140 K with another heavily damped mode with a bare frequency of 13 cm^{-1} (in analogy to the central mode in scattering experiments). The last mode is coupled near the PT temperatures with a transverse acoustic phonon. In this way we have confirmed Volkov's model of the coupled oscillators in RS.

Our fits clearly support the conclusion of Horioka *et al.*[11] that two excitations are present in the microwave and near-millimeter spectra below 30 cm^{-1} and above 140 K. This is in contrast to Volkov and co-workers,[9,10,19] who could describe the near-millimeter spectra by a single excitation only.

Accordingly, the PT in RS at T_{C1} is not a consequence of the slowing down of one relaxation as in other materials with order-disorder PT's, but it is originally caused by the softening of an optical phonon at $\sim$ 75 cm^{-1}. In this sense the PT's in RS can be treated as a hybrid between displacive and order-disorder type, but the triggering mechanism is the softening of an optical phonon. A similar situation appears to be the case with several other ferroelectric PT's,[19] as in tris-sarcosine calcium chloride,[30] gadolinium molybdate,[31] and practically all perovskite ferroelectrics.[32]

ACKNOWLEDGMENTS

The authors thank M. Horioka and H. Yanagihara for kindly providing their microwave data of RS, A. A. Volkov for providing unpublished near-millimeter data in the vicinity of T_{C1} and T_{C2}, and J. Kraus for the experimental help. One of us (S.K.) acknowledges the Alexander von Humboldt-Stiftung for financial support.

---

* On leave from the Institute of Physics, Czech Academy of Sciences, Na Slovance 2, 180 40 Prague 8, Czech Republic. Electronic address: Kamba@fzu.cz

[1] J. Valasek, Phys. Rev. **17**, 475 (1921).
[2] *Crystal and Solid State Physics*, edited by K. H. Hellwege and A. M. Hellwege, Landolt-Börnstein, New Series, Group III, Vols. 3, 9, and 16 (Springer-Verlag, Berlin, 1969, 1975, and 1982).
[3] C. A. Beevers and W. Hughes, Proc. R. Soc. London Ser. A **177**, 251 (1941).
[4] B. C. Frazer, J. Phys. Soc. Jpn. **17**, Suppl. B-II, 376 (1962).
[5] Y. Iwata, S. Mitani, and I. Shibuya, Ferroelectrics **107**, 287 (1990).
[6] H. Akao and T. Sasaki, J. Chem. Phys. **23**, 2210 (1955).
[7] H. E. Müser and J. Pottharst, Phys. Status Solidi **24**, 109 (1967).
[8] F. Sandy and R. V. Jones, Phys. Rev. **168**, 481 (1968).
[9] A. A. Volkov, G. V. Kozlov, E. B. Kryukova, and J. Petzelt, Sov. Phys. JETP **63**, 110 (1986).
[10] A. A. Volkov, G. V. Kozlov, E. B. Kryukova, and A. A. Sobyanin, Sov. Phys. Solid State **28**, 444 (1986).
[11] M. Horioka, Y. Satuma, and H. Yanagihara, J. Phys. Soc. Jpn. **62**, 2233 (1993).
[12] M. Malineau, P. Strimer, and A. Hadni, J. Chim. Phys. **2**, 243 (1972).
[13] X. Gerbaux, A. Hadni, and A. Kitade, Phys. Status Solidi A **115**, 587 (1989).
[14] I. F. Viblyi, N. A. Romanyuk, and V. V. Turkevich, Opt. Spectrosk. **34**, 521 (1973) [Opt. Spectrosc. **34**, 298 (1973)].
[15] A. N. Baker and D. S. Webber, J. Chem. Phys. **27**, 689 (1957).
[16] V. Winterfeldt, Phys. Status Solidi B **100**, 235 (1980).
[17] W. Taylor, D. J. Lockwood, and H. J. Labbe, J. Phys. C **17**, 3685 (1984).
[18] R. Bhattacharjee, Y. S. Jain, G. Raghubanshi, and H. D. Bist, J. Raman Spectrosc. **19**, 51 (1988).
[19] J. Petzelt, G. V. Kozlov, and A. A. Volkov, Ferroelectrics **73**, 101 (1987).
[20] G. A. Samara and P. S. Peercy, in *Solid State Physics Advances in Research and Applications*, edited by H. Ehrenreich, F. Seitz, and D. Turnbull (Academic Press, New York, 1981), Vol. 36, p. 1.
[21] F. Abelès, *Optical Properties of Solids* (North-Holland Publishing Company, Amsterdam, 1972), pp. 24–26.
[22] L. T. Latush, L. M. Rabkin, V. I. Torgashev, Yu. I. Yuzyuk, L. A. Shuvalov, and N. M. Schagina, Ferroelectrics **75**, 455 (1987).
[23] E. F. Ushatkin, V. V. Meriakri, and Yu. M. Poplavko, JETP Lett. **19**, 293 (1974).
[24] K. Imai, J. Phys. Soc. Jpn. **41**, 1811 (1976).
[25] N. Kaneko, M. Kaneko, and H. Takahashi, Spectrochim. Acta **40A**, 33 (1984).
[26] M. Horioka and H. Yanagihara (unpublished results).
[27] A. A. Volkov, G. V. Kozlov, and S. P. Lebedev, Sov. Phys. JETP **52**, 722 (1980).
[28] G. V. Kozlov, E. B. Kryukova, S. P. Lebedev, and A. A. Sobyanin, Sov. Phys. JETP **67**, 1689 (1988).
[29] H. Müller, Phys. Rev. **58**, 565 (1940).
[30] J. Petzelt, A. A. Volkov, Yu. G. Goncharov, J. Albers, and A. Klöpperpieper, Solid State Commun. **73**, 5 (1990).
[31] J. Petzelt, F. Smutný, V. Katkanant, F. G. Ullman, J. R. Hardy, A. A. Volkov, G. V. Kozlov, and S. P. Lebedev, Phys. Rev. B **30**, 5172 (1984).
[32] M. D. Fontana, H. Idrissi, and K. Wojcik, Europhys. Lett. **11**, 419 (1990).